

# Oxygen doping of P3HT:PCBM blends: Influence on trap states, charge carrier mobility and solar cell performance

Julia Schafferhans <sup>1,\*</sup> Andreas Baumann <sup>1</sup>, Alexander Wagenpohl <sup>1</sup>, Carsten Deibel <sup>1</sup>, and Vladimir Dyakonov <sup>1,2†</sup>

<sup>1</sup> *Experimental Physics VI, Faculty of Physics and Astronomy,*

*Julius-Maximilians-University of Würzburg, Am Hubland, 97074 Würzburg, Germany and*

<sup>2</sup> *Bavarian Center of Applied Energy Research e.V. (ZAE Bayern), Am Hubland, 97074 Würzburg, Germany*

We investigated the influence of oxygen on the performance of P3HT:PCBM (poly(3-hexylthiophene):[6,6]-phenyl C61 butyric acid methyl ester) solar cells by current–voltage, thermally stimulated current (TSC) and charge extraction by linearly increasing voltage (CELIV) measurement techniques. The exposure to oxygen leads to an enhanced charge carrier concentration and a decreased charge carrier mobility. Further, an enhanced formation of deeper traps was observed, although the overall density of traps was found to be unaffected upon oxygen exposure. With the aid of macroscopic simulations, based on solving the differential equation system of Poisson, continuity and drift-diffusion equations in one dimension, we demonstrate the influence of a reduced charge carrier mobility and an increased charge carrier density on the main solar cell parameters, consistent with experimental findings.

## 1. INTRODUCTION

Power conversion efficiencies of almost 8% for organic solar cells have already been achieved, with growing tendency [1]. A critical issue yet to be addressed are the factors influencing the device lifetime. To gain a detailed understanding of the device stability, as well as the underlying degradation mechanisms and their impact on the solar cell performance is an important prerequisite for lifetime enhancements.

Organic solar cells undergo many degradation pathways during their lifetime. Efficiency losses due to light [2], oxygen [3, 4] and water [5] are reported. The details of the degradation processes, however, are still not completely understood. Other studies, on the contrary, are only focused on the degradation of a single active material instead of the blend. For example for P3HT oxygen is known to form a charge transfer complex [6] resulting in p-doping of P3HT [7, 8], which is also investigated theoretically by band-structure calculations [9]. Furthermore, oxygen induced degradation of P3HT is reported to result in decreased mobilities [6, 10] and increased trap densities [10]. In the case of C60, oxygen also causes decreased electron mobilities [11, 12] and increased trap densities [13], as demonstrated by investigations of C60 based field effect transistors.

This paper addresses the oxygen induced degradation of poly(3-hexylthiophene):[6,6]-phenyl C61 butyric acid methyl ester solar cells in the dark, as well as under simultaneous illumination. Detailed investigations including charge carrier mobility, charge carrier density and defect spectroscopic measurements are performed to get an insight of the degradation mechanism due to oxygen in P3HT:PCBM solar cells.

## 2. EXPERIMENTAL

The investigated bulk heterojunction solar cells were prepared by spin coating P3HT:PCBM (ratio 1:0.8) blends made from solutions of 30 mg/ml in chlorobenzene on poly(3,4-ethylenedioxythiophene) poly(styrenesulfonate) (Pedot:PSS) covered indium tin oxide/glass substrates. The active layer was about 240 nm thick. After an annealing step of 10 min at 130 °C, Ca (1.5nm)/Al (60nm) contacts were evaporated thermally (base pressure during evaporation  $< 7 \cdot 10^{-7}$  mbar). The effective areas of the solar cells were 3 mm<sup>2</sup> and 9 mm<sup>2</sup>.

PEDOT:PSS was purchased by H.C.Starck (CLEVIOS P VP Al 4083). P3HT was delivered by BASF (Sepiolid P200), PCBM (purity 99,5 %) by Solenne. All materials were used without further purification. All preparation steps were performed in a nitrogen glovebox and an attached thermal vacuum evaporation chamber.

Initial current–voltage (IV) characteristics of the solar cells were measured in the nitrogen glovebox. For the illumination of the cells we used an Oriel 81160 AM1.5G solar simulator. The power conversion efficiencies of the investigated samples were 3% – 3.5%.

Degradation studies of the unprotected solar cells were performed in a closed cycle cryostat. During the thermally stimulated current (TSC), charge carrier extraction by linearly increasing voltage (CELIV) [14, 15] and IV-measurements the cryostat was filled with helium as contact gas. To investigate the influence of oxygen on the solar cells, the helium was replaced with synthetic air (80% N<sub>2</sub>, 20% O<sub>2</sub>,  $< 1$ ppm H<sub>2</sub>O) for different degradation times. Thus, the effect of humidity was excluded. This exposure was always done at a constant temperature of 300 K. Two different degradation conditions were investigated: in synthetic air either in the dark or under illumination. For the latter we used a 10 W high power white light emitting diode (Seoul). The light intensity was adjusted to match the short circuit current of the non degraded cells obtained under the solar simulator.

\*Electronic mail: julia.schafferhans@physik.uni-wuerzburg.de

†Electronic mail: dyakonov@physik.uni-wuerzburg.de

The LED was also used for the illuminated IV-curves in the cryostat.

For TSC measurements the trap filling was achieved by illumination of the samples at 18 K for five minutes using the 10 W LED. After a dwell time of five minutes the temperature was increased with a constant heating rate of 7 K/min up to 300 K. The TSC signals were detected by a Sub-Femtoamp Remote Source Meter (Keithley 6430) without applying an external field, implying that the de-trapped charge carriers were extracted from the samples only due to the built-in voltage. Further details of the TSC measurements are described elsewhere [10].

CELIV measurements were performed at 300 K. The peak voltage of the triangular bias pulse in reverse direction was  $V_a = 2$  V applied on the Ca/Al electrode. A voltage pulse width of 50  $\mu$ s was chosen.

### 3. RESULTS AND DISCUSSION

#### 3.1. Experimental Results

The IV-curves for different degradation times between

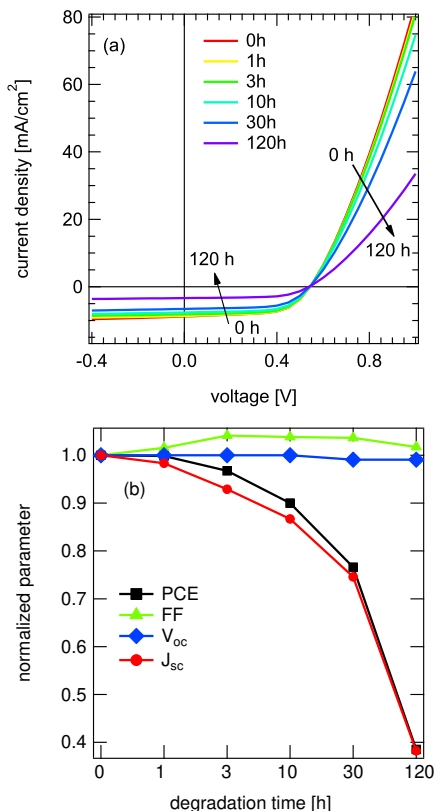


FIG. 1: Illuminated IV-curves of P3HT:PCBM solar cells for different dark degradation times in synthetic air (a) and the normalized values of the PCE, fill factor, open circuit voltage and short circuit current (b). The efficiency loss is due to the decrease of the short circuit current.

0 h and 120 h in synthetic air in the dark are shown in Fig. 1a. The obtained values for the power conversion efficiency (PCE), fill factor (FF), open circuit voltage ( $V_{oc}$ ) and short circuit current ( $J_{sc}$ ), normalized to the initial values are presented in Fig. 1b. The observed efficiency loss with dark degradation time is only due to  $J_{sc}$ , which decreases about 60% within 120 h, whereas  $V_{oc}$  and FF remain almost constant. Since the exposure of the samples to synthetic air in the dark results only in a loss in  $J_{sc}$ , a degradation of the electrodes being the origin of these findings can be excluded. Degradation (oxidation) of the Ca/Al electrode would result in the occurrence of an s-shaped IV-curve [16], at least in a strong loss in FF or  $V_{oc}$ . Neither of these effects was observed within the timescale of degradation considered here.

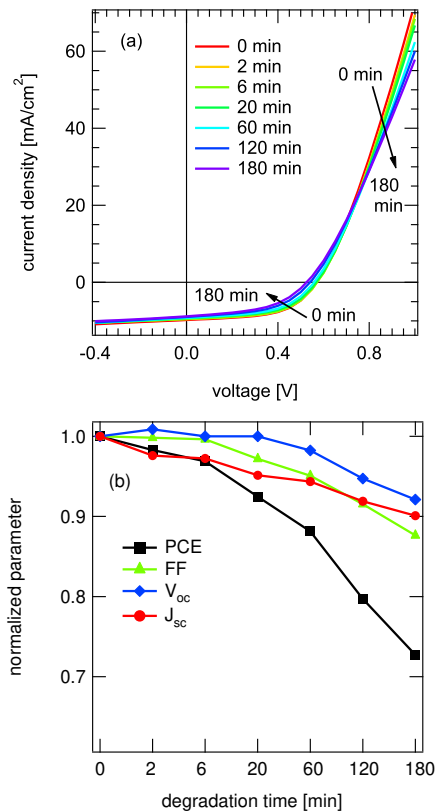


FIG. 2: Illuminated IV-curves of P3HT:PCBM solar cells for different degradation times in synthetic air under simultaneous illumination (a) and the normalized values of the PCE, fill factor, open circuit voltage and short circuit current (b). In contrast to dark degradation in synthetic air all parameters decrease.

In contrast to degradation in synthetic air in the dark, the efficiency loss due to degradation in synthetic air and simultaneous illumination (Fig. 2a, b) occurs on a faster time scale—about 30% efficiency loss within 180 min—and is caused by a decrease of  $J_{sc}$ , as well as FF and  $V_{oc}$ , which all decrease about 10% within this time scale. Since, in the case of dark degradation, FF and  $V_{oc}$  are unaffected, the decrease of both during photodegrada-

tion is due to light in the presence of oxygen, indicating an additional degradation path due to photooxidation in addition to doping as found under oxygenation in the dark.

To gain a deeper understanding of the underlying degradation mechanisms, we performed TSC measurements to obtain information about the electronic trap states of P3HT:PCBM solar cells for dark as well as photodegradation. First of all, the trap distribution of non degraded P3HT:PCBM solar cells was investigated by applying a fractional TSC measurement—the so-called  $T_{start}$ - $T_{stop}$  technique [10, 17]—with  $T_{stop}$  varied between 25 K and 150 K in steps of 5 K. The resulting density of occupied states (DOOS) distribution is shown in Fig. 3. The continuous activation energies of the traps

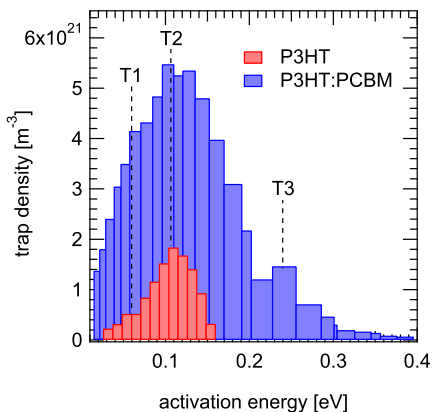


FIG. 3: Comparison of the DOOS distribution of P3HT and P3HT:PCBM blends, as obtained by TSC- $T_{start}$ - $T_{stop}$  measurements. The DOOS of P3HT consists of two different traps (T1, T2), which both also contribute to the DOOS of the blend. Additionally to these two traps the DOOS of the blend features a third trap distribution (T3) with higher activation energy.

range from 20 meV to 400 meV with the center of distribution at about 105 meV. For further interpretation of the DOOS distribution of the blend, we consider the results for pure P3HT. For P3HT, the DOOS was related to two different overlapping traps with approximately Gaussian energy distributions [10], with the center of distribution of the dominant trap at about 105 meV (T2) and the other at about 50 meV (T1) (shoulder at the low energy side of the DOOS distribution) (Fig. 3). Since the centers of distribution for the blend as well as the pure P3HT are at 105 meV, we attribute the dominant trap to P3HT, although the distribution of the main trap in the blend is broadened as compared to the pure P3HT, indicating a higher disorder in the blend. Furthermore, the T1 can also be seen in the DOOS distribution of the blend in the steep onset of the distribution on the low energy side, but is less pronounced due to the higher concentration of the main trap T2, overlapping T1. Additionally to these two traps, the DOOS distribution of the blend features further trap states with activation energies of

200 meV to 400 meV which are not seen in pure P3HT, with the center at about 250 meV. We refer to the latter trap distribution as T3. Therefore we conclude that the DOOS of the blend consists of three different traps, with the dominant trap T2 at 105 meV. This interpretation is also supported by the TSC spectrum of pristine P3HT:PCBM solar cells, where T2 has a lower concentration compared to T1 and T3, so that T1, T2, and T3 can be clearly distinguished (data not shown). The trap density obtained from the TSC measurements of the investigated P3HT:PCBM solar cells is in the range of  $6 - 8 \cdot 10^{22} \text{ m}^{-3}$  which is considerably higher than the value obtained for P3HT ( $1 \cdot 10^{22} \text{ m}^{-3}$ ) [10].

The TSC spectra of P3HT:PCBM solar cells for different dark degradation times in synthetic air are shown in Fig. 4a. Thermally stimulated current is observed

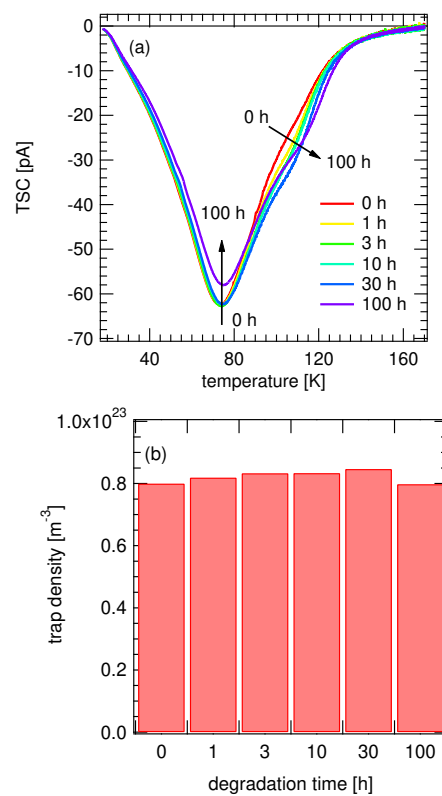


FIG. 4: TSC spectra of P3HT:PCBM solar cells for different dark degradation times in synthetic air (a) and the obtained trap densities (b). The trap density remains almost constant. The slight decrease of the trap density for 100 h degradation time is possibly due to recombination of the detrapped charge carriers.

between 18 K and 160 K. At higher temperatures no additional TSC peaks can be observed up to 300 K. With exposure to synthetic air, a shoulder at about 100 K appears, which increases with longer degradation times within the investigated time scale up to 100 h. The appearance of a shoulder indicates an increase in density of the deeper traps or even the formation of additional traps. The main peak however decreases slightly. As a

result the overall trap density of the blend obtained by the TSC measurements remains almost constant for the different degradation times (Fig. 4b). In this context it has to be mentioned that the determined trap density from the TSC spectra is only a lower limit of the actual trap density [18]. One reason is a possible recombination between electrons and holes after one of them got trapped due to thermal activation. For degradation on synthetic air and simultaneous illumination we monitored

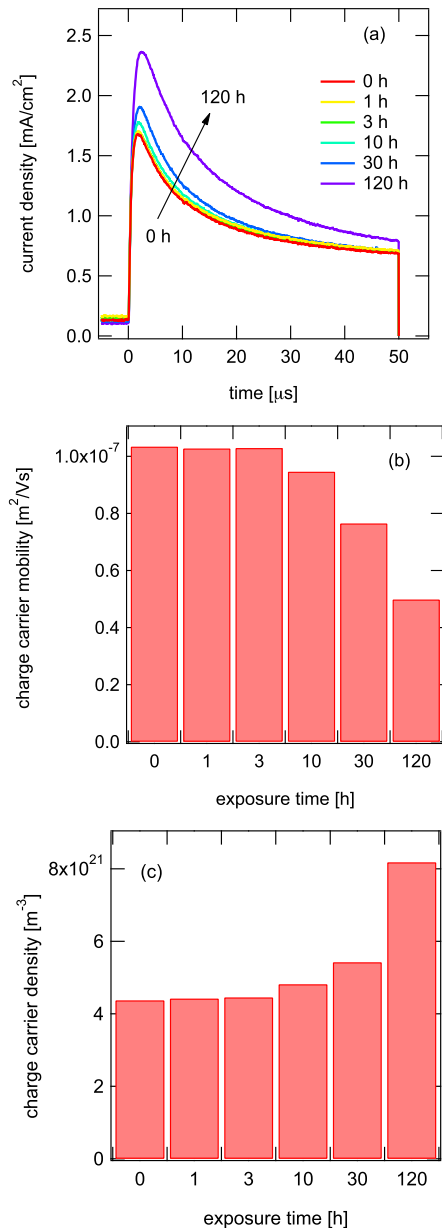


FIG. 5: CELIV measurements of P3HT:PCBM solar cells for different dark degradation times in synthetic air for offset bias of  $-0.3$  V applied at the Ca/Al electrode (a) and the obtained mobilities (b) as well as the charge carrier densities (c). The charge carrier mobility slightly decreases with degradation time, whereas the charge carrier density shows an increase due to oxygen doping.

almost the same behavior of TSC spectra, but on a faster timescale than during dark degradation.

To get further information about the influence of oxygen on the mobility and also the charge carrier concentration of the blend, we used the CELIV technique, which enables the simultaneous investigation of equilibrium charge carrier density and mobility by recording transient currents. The CELIV measurements for different degradation times in synthetic air in the dark are shown in Fig. 5a. The CELIV curves exhibit a high asymmetry, especially for longer degradation times, which might result from trapped charge carriers being extracted as the higher voltages at longer times promote emission from traps. This is in accordance with the increase of the deeper traps density as revealed by the TSC measurements. The mobility for different degradation times was calculated from the position of the current peak maximum according to reference [15]. Only a slight decrease of the mobility with degradation time can be observed (Fig. 5b), resulting in a decrease of about 50 % after 120 h in synthetic air. The equilibrium charge carrier density, extracted by the CELIV measurements, however, increases about a factor of two within a degradation time of 120 h in the dark (Fig. 5c). We assign these additional charge carriers to oxygen doping of P3HT, which was also reported for P3HT diodes [10] and P3HT field effect transistors [7, 8]. We note that the concentration of charges measured by CELIV provides only a lower limit of the actual charge carrier density, since only charge carriers extracted within the time scale of the experiment (voltage pulse width typically 50  $\mu$ s) are observed. Thus, the experimental number includes charges from comparably shallow traps which can be emitted from them and then be extracted; charges in deeper traps as well as the ones lost within the sample (by recombination) are disregarded. The degradation on synthetic air and simultaneous illumination shows similar results for the changes in mobility and charge carrier concentration, but again the degradation is accelerated to a timescale of minutes instead of hours.

### 3.2. Simulation

In order to understand the influence of a decreased mobility as well as charge carrier doping on the solar cell parameters, we performed macroscopic simulations based on solving the differential equation system of the Poisson, the continuity and the drift-diffusion equations in one dimension [19, 20]. In the simulation we accounted a bimolecular non-geminate recombination rate according to Langevin [21]. The charge carrier generation by light was assumed to create free polarons, neglecting any influence of electric field driven polaron pair dissociation. Furthermore the charge carrier mobilities of electrons and holes were set equal in the simulations. The used parameters are listed in Table I. Using this approach we investigated the effect of charge carrier doping by oxygen on the solar

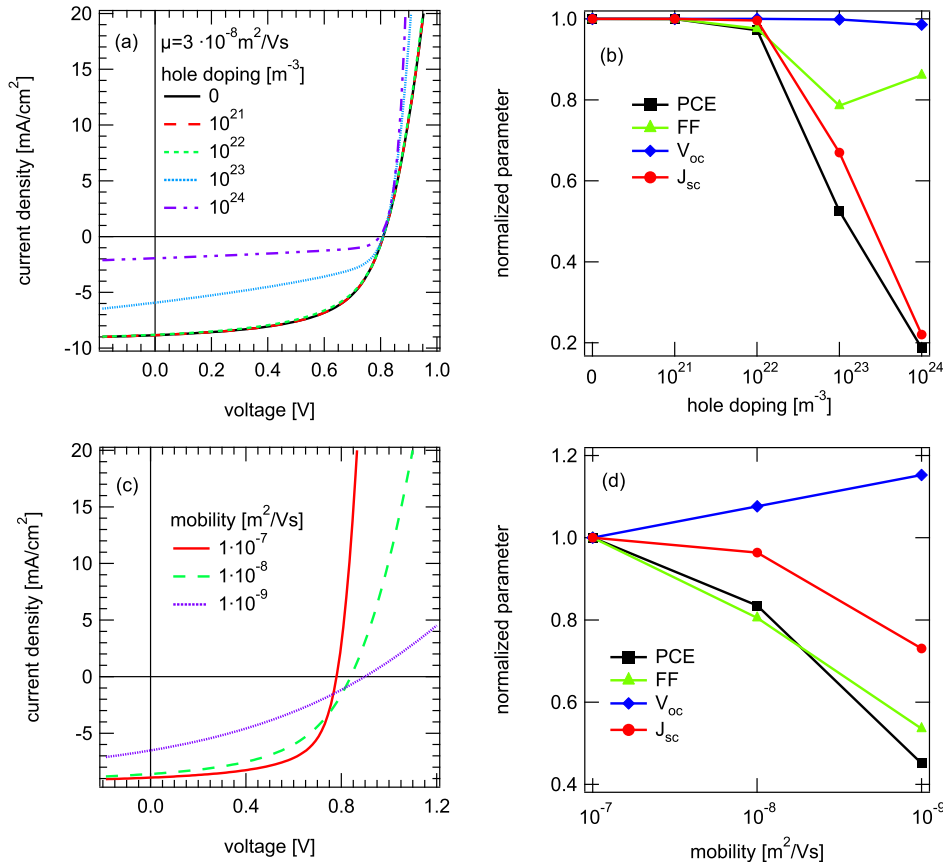


FIG. 6: Simulated IV-curves for different levels of hole doping (a) and the normalized values of the PCE, fill factor, open circuit voltage and short circuit current (b). An increased doping level results in a decrease of  $J_{sc}$ . A lowered charge carrier mobility (c) instead leads to a decrease of  $J_{sc}$  and FF (d).

parameter	symbol	value	unit
temperature	$T$	300	K
effective band gap	$E_g$	1.30	eV
relative dielectric constant	$\epsilon_r$	3.6	
active layer thickness	$L$	100	nm
effective density of states	$N_c, N_v$	$8.0 \times 10^{25}$	$1/m^3$
generation rate	$G$	$6.0 \times 10^{27}$	$1/m^3s$
injection barriers	$\Phi_a, \Phi_c$	0.1	eV

TABLE I: Parameters used for simulation.

cell parameters.

The simulated IV-curves for different hole doping levels are shown in Fig. 6 a and the corresponding normalized solar cell parameters in Fig. 6 b. For the given parameter set, doping concentration up to  $10^{22} m^{-3}$  does not change the PCE, whereas for higher concentrations the PCE strongly decreases due to a decrease of  $J_{sc}$ . FF and  $V_{oc}$ , however, remain almost unaffected. This behavior is almost independent of the mobility (within changes of one order of magnitude) used for the simulations. The decreased  $J_{sc}$  due to doping can be explained

by an increased bimolecular recombination probability. Since doping implies additional charges within the device, it leads to less band bending and therefore a reduced electrical field within the solar cell. As a consequence the extraction time for the charge carriers increases leading to a higher recombination probability and thus to a lower short circuit current.

The influence of the mobility on the solar cell performance is shown in Fig. 6 c, d, revealing a loss of  $J_{sc}$  and FF and a small increase of  $V_{oc}$  for decreased mobilities. A lower mobility leads to a higher extraction time for the charge carriers and therefore to an enhanced bimolecular recombination probability, which results in the decreased FF. At the same time, the charge extraction becomes less efficient. The slightly increasing open circuit voltage is due to a lower Langevin recombination rate due to decreased mobilities. The higher charge carrier densities and their more balanced distribution reduce the internal electric field and therefore increase the open circuit voltage[22, 23]. If the field dependent polaron pair dissociation was also taken into account, it would mostly influence the FF and  $J_{sc}$  resulting in an even stronger decrease with lower mobilities.

### 3.3. Discussion

The influence of oxygen on P3HT:PCBM solar cells results in the case of dark degradation in a loss of  $J_{sc}$ , whereas photodegradation results in a decrease of all solar cell parameters. Further, the degradation due to oxygen is accelerated by light. A similar behavior was recently reported for inverted P3HT:PCBM solar cells [3], where the efficiency yields almost no change for dark degradation within the investigated timescale of 1h, whereas a strong loss for photodegradation within 120 min is observed. The loss in  $J_{sc}$  can be explained by charge carrier doping, as we demonstrated by using macroscopic simulations. This interpretation is in accordance with the CELIV measurements, which show an increasing charge carrier concentration with degradation time. We attribute the increased charge carrier concentration to oxygen doping of P3HT [7, 8, 10]. The difference between the doping levels in the simulations and these determined by CELIV can be explained by the fact that the extracted charge carrier density by CELIV is only a lower limit of the actual charge carrier concentration, as mentioned before. The actual charge carrier density can be significantly higher. Furthermore, the accelerated increase of the charge carrier density in the case of photodegradation compared to the dark degradation is in good agreement with results of P3HT transistors, which also showed an expedited oxygen doping with light [7].

In addition to an increased charge carrier concentration, CELIV measurements reveal a decrease of the charge carrier mobility for the P3HT:PCBM blends due to oxygen. A decreasing mobility with degradation time is also reported for pure P3HT [10], but in contrast to pure P3HT, where the mobility decreases about two orders of magnitude within 100 h [10], only a slight decrease in the blend—by about 50 %—can be observed. This difference could be due to a stabilization effect of PCBM for P3HT in analogy to findings for MDMO-PPV (poly(2-methoxy-5-(3',7'-dimethyloctyloxy)-1,4-phenylene-vinylene)):PCBM solar cells [4]. The decreased mobility could also result from a degradation of PCBM due to oxygen. Decreased electron mobilities for C60 based field effect transistors after oxygen exposure have already been reported [11, 12]. Since electron and hole mobilities can not be discriminated by CELIV, it is not possible to resolve which carrier mobility decreases.

A lower mobility leads to a decrease of FF and  $J_{sc}$ , as revealed by macroscopic simulations. Although our CELIV measurements show a slight decrease in mobility with degradation time, there are some facts indicating that the decreased mobility is not the origin of the FF loss in the case of photodegradation. First of all the experimentally observed mobility reduction is too limited to have a strong impact on the FF. Furthermore, the mobility decreases in the same range for both dark and illuminated degradation, although the degradation in the

illuminated case occurs on a faster timescale. In contrast, the loss in FF is only observed for photodegradation. Additionally, we experimentally observed also a decrease of  $V_{oc}$  for photodegradation, whereas a decrease in mobility should result in an increase of  $V_{oc}$  as exhibited by the simulation (Fig. 6 d). Therefore, the decreased mobility is not the reason for the FF loss.

Another important factor which can negatively influence the solar cell performance are electronic trap states, since they lower the mobility, disturb the internal field distribution and can act as recombination centers. Exposure of P3HT:PCBM solar cells to oxygen results in a rise of the density of deeper traps for both dark and illuminated degradation. On the other hand, the main peak of the TSC slightly decreases due to oxygen exposure, which is in contrast to the observed increase of the main TSC peak of pure P3HT [10]. For comparison, the trap density in pure P3HT increases almost by a factor of three within 100 h under oxygen exposure [10]. In this context we want to mention again that the determined trap density from the TSC spectra is only a lower limit of the actual trap density [18].

The appearance of deeper traps due to oxygen exposure could also be the reason for the observed loss in fill factor, since they can disturb the internal field distribution and act as recombination centers, as mentioned before. Further investigations concerning the influence of deep traps on the solar cell performance have to be done, like the implementation of deep traps within the macroscopic simulation. Other crucial factors concerning FF and  $V_{oc}$  we want to address, are imbalanced electron–hole mobilities (resulting in the formation of space charges) and a field dependent photogeneration. These two factors have not been accounted so far and will be addressed in the future to completely clarify the origin of the loss of FF and  $V_{oc}$  in the case of oxygen induced degradation under simultaneous illumination.

## 4. CONCLUSIONS

We investigated the influence of oxygen on unprotected P3HT:PCBM solar cells by controlled exposure to synthetic air. Two different degradation conditions were used: in the dark and under simultaneous illumination. Exposure of the solar cells to synthetic air in the dark results in a loss of  $J_{sc}$  of about 60 % within 120 h. In contrast, simultaneous illumination during oxygen degradation results in a loss of all solar cell parameters, yielding an efficiency loss of about 30 % within only 3 hours. Thus, the degradation of the P3HT:PCBM solar cells is strongly accelerated by light.

CELIV measurements revealed an increased charge carrier concentration after oxygen exposure for dark, as well as photodegradation. We attributed these additional charge carriers to oxygen doping, which is also known for pure P3HT. With the aid of macroscopic simulations we have shown that doping of the solar cells is the origin of

the loss in  $J_{sc}$  for both degradation conditions.

Another impact of oxygen exposure on P3HT:PCBM solar cells is a slight decrease of the charge carrier mobility, as also revealed by CELIV measurements. Although a decreased mobility may result in a loss of the fill factor, as shown by macroscopic simulations, the experimentally observed mobility decrease is too small to be the origin of the FF drop in the case of photodegradation.

In addition to an enhanced charge carrier concentration, oxygen induced degradation results in an increase of the density of deeper traps, as was revealed by TSC measurements. These deep traps could be the origin of the decreased FF and  $V_{oc}$ , although further investigations to correlate the trap density to the solar cell performance are required for a verification.

## Acknowledgements

The current work is supported by the Bundesministerium für Bildung und Forschung in the framework of the OPV Stability Project (Contract No. 03SF0334F). J.S. thanks the Elitenetzwerk Bayern for funding. A.B. thanks the Deutsche Bundesstiftung Umwelt for funding. C.D. gratefully acknowledges the support of the Bavarian Academy of Sciences and Humanities. V.D.'s work at the ZAE Bayern is financed by the Bavarian Ministry of Economic Affairs, Infrastructure, Transport and Technology. The authors thank Jens Lorrman for fruitful discussion.

- 
- [1] M. A. Green, K. Emery, Y. Hishikawa, W. Warta, Solar cell efficiency tables (version 35), *Prog. Photovolt: Res. Appl.* 18 (2010) 144.
- [2] M. O. Reese, A. J. Morfa, M. S. White, N. Kopidakis, S. E. Shaheen, G. Rumbles, D. S. Ginley, Pathways for the degradation of organic photovoltaic P3HT:PCBM based devices, *Sol. Ener. Mat. Sol. Cells* 92 (2008) 746.
- [3] A. Seemann, H.-J. Egelhaaf, C. J. Brabec, J. A. Hauch, Influence of oxygen on semi-transparent organic solar cells with gas permeable electrodes, *Org. Electron.* 10 (2009) 1424.
- [4] H. Neugebauer, C. Brabec, J. C. Hummelen, N. S. Sariciftci, Stability and photodegradation mechanisms of conjugated polymer/fullerene plastic solar cells, *Sol. Ener. Mat. Sol. Cells* 61 (2000) 35.
- [5] K. Norrman, S. A. Gevorgyan, F. C. Krebs, Water-induced degradation of polymer solar cells studied by H218O labeling, *Applied Materials and Interfaces* 1 (2009) 102.
- [6] M. S. A. Abdou, F. P. Orfino, Y. Son, S. Holdcroft, Interaction of oxygen with conjugated polymers: Charge transfer complex formation with poly(3-alkylthiophene), *J. Am. Chem. Soc.* 119 (1997) 4518.
- [7] H.-H. Liao, C.-M. Yang, C.-C. Liu, S.-F. Horng, H.-F. Meng, J.-T. Shy, Dynamics and reversibility of oxygen doping and de-doping for conjugated polymer, *J. Appl. Phys.* 103 (2008) 104506.
- [8] E. J. Meijer, C. Detcheverry, P. J. Baesjou, E. van Veenendaal, D. M. de Leeuw, T. M. Klapwijk, Dopant density determination in disordered organic field-effect transistors, *J. Appl. Phys.* 93 (2003) 4831.
- [9] C.-K. Lu, H.-F. Meng, Hole doping by molecular oxygen in organic semiconductors: Band-structure calculations, *Phys. Rev. B* 75 (2007) 235206.
- [10] J. Schafferhans, A. Baumann, C. Deibel, V. Dyakonov, Trap distribution and the impact of oxygen-induced traps on the charge transport in poly(3-hexylthiophene), *Appl. Phys. Lett.* 93 (2008) 093303.
- [11] A. Tapponnier, I. Biaggio, P. Günter, Ultrapure C60 field-effect transistors and the effects of oxygen exposure, *Appl. Phys. Lett.* 86 (2005) 112114.
- [12] R. Könenkamp, G. Priebe, B. Pietzak, Carrier mobilities and influence of oxygen in C60 films, *Phys. Rev. B* 60 (1999) 11804.
- [13] T. Matsushima, M. Yahiro, C. Adachi, Estimation of electron traps in carbon-60-field-effect transistors by a thermally stimulated current technique, *Appl. Phys. Lett.* 91 (2007) 103505.
- [14] G. Juška, K. Arlauskas, M. Viliūnas, J. Kočka, Extraction current transients: New method of study of charge transport in microcrystalline silicon, *Phys. Rev. Lett.* 84 (2000) 4946.
- [15] C. Deibel, Charge carrier dissociation and recombination in polymer solar cells, *Phys. Stat. Sol. A* 206 (2009) 2731.
- [16] A. Wagenpfahl, D. Rauh, M. Binder, C. Deibel, V. Dyakonov, On the s-shape current-voltage characteristics of organic solar devices, arXiv:1005.5669v1 (2010).
- [17] R. Schmechel, H. von Seggern, Electronic traps in organic transport layers, *Phys. Stat. Sol. A* 201 (2004) 1215.
- [18] A. Kadashchuk, R. Schmechel, H. von Seggern, U. Scherf, A. Vakhnin, Charge-carrier trapping in polyfluorene-type conjugated polymers, *J. Appl. Phys.* 98 (2005) 024101.
- [19] C. Deibel, A. Wagenpfahl, V. Dyakonov, Influence of charge carrier mobility on the performance of organic solar cells, *Phys. Stat. Sol. (RRL)* 2 (2008) 175.
- [20] C. Deibel, A. Wagenpfahl, V. Dyakonov, Origin of reduced polaron recombination in organic semiconductor devices, *Phys. Rev. B* 80 (2009) 075203.
- [21] P. Langevin, Recombinaison et mobilités des ions dans les gaz, *Ann. Chim. Phys.* 28 (1903) 433.
- [22] L. J. A. Koster, V. D. Mihailetschi, R. Ramaker, P. W. M. Blom, Light intensity dependence of open-circuit voltage of polymer:fullerene solar cells, *Appl. Phys. Lett.* 86 (2005) 123509.
- [23] D. Cheyons, J. Poortmans, P. Heremans, C. Deibel, S. Verlaak, B. P. Rand, J. Genoe, Analytical model for the open-circuit voltage and its associated resistance in organic planar heterojunction solar cells, *Phys. Rev. B* 77 (2008) 165332.